UNIVERSITY of CALIFORNIA
SANTA CRUZ

**VECTOR BOSON SCATTERING**

A thesis submitted in partial satisfaction of the
requirements for the degree of

BACHELOR OF SCIENCE

in

PHYSICS

by

**Adrian Thompson**

11 June 2015

The thesis of Adrian Thompson is approved by:

| | |
|---|---|
| Professor Jason Nielsen<br>Advisor | Professor Adriane Steinacker<br>Theses Coordinator |

Professor Robert Johnson
Chair, Department of Physics

**Abstract**

Vector Boson Scattering

by

Adrian Thompson

The theory of a complex scalar Higgs field which provides a mechanism for electroweak symmetry breaking (EWSB) is outlined to provide motivation for the study of the electroweak sector through vector boson scattering (VBS). Many of the exact mechanisms of EWSB have yet to be confirmed in the TeV scale, where the existence of new physics is sought after as a source of unitarity preservation. The use of an effective field theory as a way of incorporating anomalous couplings of new physics is presented as a modern way to study EWSB beyond the standard model.

# Contents

# Acknowledgements

Professor Jason Nielsen, for his kindness, zeal, and continuous guidance of my physics research.

Professor Adriane Steinacker, for her passion and encouragement towards my success as a physics student.

Professor Howard Haber, whose mentoring in this topic helped greatly.

Niklas Garner, Alden Deran, and Oscar Flores, who were the greatest fellow colleagues to work with.

Mom and Dad.

*"Nature is the great visible engine of creativity, against which all other creative efforts are measured."*

Terrence McKenna

# 1

# Introduction

The electroweak sector of particle physics provides a rich vein for the research of EWSB and the Higgs mechanism [1], [2],[11]. Electroweak symmetry breaking is a spontaneous symmetry breaking of the Higgs potential, and it is the origin of the vector boson mass eigenstates as they are now, which are actually linear superpositions of more fundamental fields. Since the symmetry breaking is spontaneous, there is currently no way of predicting how the symmetry gets broken. To access the effects of EWSB related phenomena, particle collisions with exceedingly high beam energies and luminosities are required. At particle energies of hundreds of GeV, the Higgs field lies at the center of our focus. The Higgs endows elementary particles with mass, couples to the longitudinal modes of the massive vector bosons, and plays a part in the unitarization of electroweak processes. For these reasons, it is a worthy task to investigate beyond the Standard Model (BSM) effects of EWSB.

Electroweak symmetry breaking occurred as a single event in the early universe,

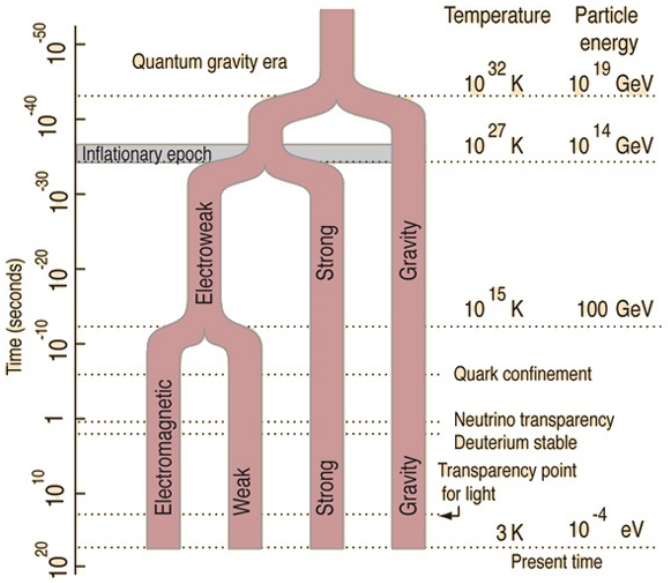


Figure 1.1: A timeline showing the decoupling of the forces from one another [24].

around $10^{-12}$ s after the Big Bang, coinciding with temperatures dropping below a critical temperature around $10^{16}$ K. The underlying mechanism is in the Higgs field attaining its ground state with a nonzero vacuum expectation value (vev). This machinery is described by the Weinberg-Salam model of electroweak theory [3], [4].

## 1.1 Weinberg-Salam Theory and the Higgs Mechanism

The following discussion can be found in any quantum field theory or particle physics textbook, and I have chosen to use Ryder [5] and the more recent book by Lancaster and Blundell [6] as guidelines. I will try to elucidate any points that are unclear and bring the discussion into a greater and more relevant context.

The Weinberg-Salam theory begins by forcing the existing fields of the universe to respect a $SU(2) \times U(1)$ (or $U(2)$) symmetry, ignoring for a moment the $SU(3)$ symmetries of the strongly interacting fields. For some context, refer to Figure 1.1, in particular the time just before $10^{-12}$ s after the Big Bang. Before this time, towards the top of the figure, the fields may have exhibited higher degrees of symmetry, e.g. under the action of $SU(5)$ [7].

The symmetry groups will yield the state of the electroweak sector at this stage. $U(1)$ symmetry implies that the Lagrangian for the lepton fields is invariant under local phase transformations like $e^{if(x)}$. There is a charge associated with this symmetry called the weak hypercharge, $Y$, which is carried by the fields. Invariance under this symmetry brings in the gauge field $B_\mu$, where $\mu \in \{0, 1, 2, 3\}$ is the spacetime index. The $SU(2)$ group gives the fields a charge vector $I$, the weak isospin, which is $\frac{1}{2}$-integral and respects the same algebra as spin angular momentum. Local invariance under $SU(2)$ symmetry is what leads to the existence of another gauge field, $W^a_\mu$, $a \in \{1, 2, 3\}$. The way these fields are introduced is through gauge transformations just like the one used for electromagnetism; $\partial_\mu \to \partial_\mu - iqA_\mu = D_\mu$. The transformation laws here give the covariant derivative $D_\mu = \partial_\mu \underbrace{-\frac{i}{2}g_1\sigma^a W^a_\mu}_{SU(2)} \underbrace{-\frac{i}{2}g_2 B_\mu}_{U(1)}$. This allows for the construction of a Lagrangian which contains the lepton fields and the mentioned gauge fields. A number of remarkable things will happen after introducing the Higgs field.

The Higgs is introduced as a complex scalar field, meaning that it is complex

valued and that it transforms as a scalar under Lorentz transformations. The rules for a general complex scalar field are well known. As an example, consider the following general field.

$$\phi = \frac{1}{\sqrt{2}}(\phi_0 + i\phi_1)$$
$$\phi^\dagger = \frac{1}{\sqrt{2}}(\phi_0 - i\phi_1)$$

The associated Lagrangian is also known;

$$\mathcal{L} = \partial^\mu \phi^\dagger \partial_\mu \phi - m^2 \phi^\dagger \phi - g(\phi^\dagger \phi)^2,$$

and it is invariant under $U(1)$ transformations. Compare this to the actual Higgs field, this time conceived as a complex scalar doublet, also known as an isospinor:

$$\Phi = \frac{1}{\sqrt{2}} \begin{pmatrix} \phi_0 + i\phi_1 \\ \\ \phi_2 + i\phi_3 \end{pmatrix}$$

$$\mathcal{L}_H = (D^\mu \Phi)^\dagger (D_\mu \Phi) + \underbrace{\frac{m_H^2}{2}\Phi^\dagger\Phi - \frac{\lambda}{4}(\Phi^\dagger\Phi)^2}_{-V(\Phi)}$$

Reading off the potential energy from $\mathcal{L}_H$ gives the Mexican hat shape (Figure 1.2). Where is the minimum of the potential?

$$V(\Phi^\dagger\Phi) = -\frac{m_H^2}{2}\Phi^\dagger\Phi + \frac{\lambda}{4}(\Phi^\dagger\Phi)^2 \tag{1.1}$$
$$\frac{\partial V}{\partial(\Phi^\dagger\Phi)} = -\frac{m_H^2}{2} + \frac{\lambda}{2}\Phi^\dagger\Phi$$
$$\frac{\partial V}{\partial(\Phi^\dagger\Phi)} = 0 \rightarrow (\Phi^\dagger\Phi)_{GS} = \frac{m_H^2}{\lambda} = v^2$$

The minimum occurs at $(\Phi^\dagger\Phi)_{GS} = \frac{1}{2}(\phi_0^2 + \phi_1^2 + \phi_2^2 + \phi_3^2) = \frac{m_H^2}{\lambda}$. With the appropriate choice of basis, the ground state can be chosen with $\phi_1 = \phi_2 = \phi_3 = 0$,

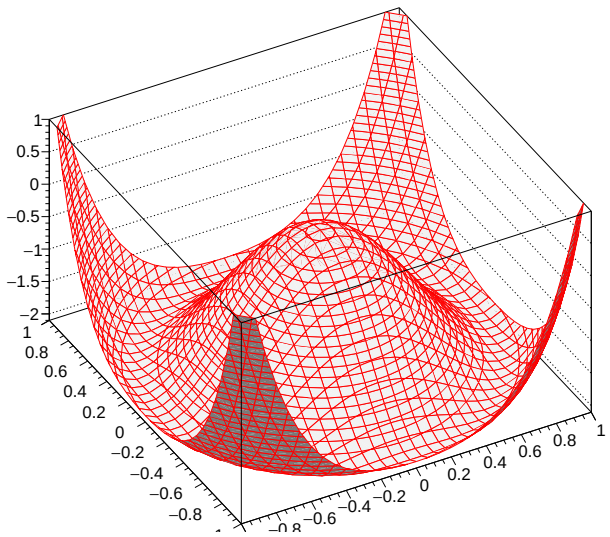


Figure 1.2: The Higgs potential. Equation 1.1 describes the functional form of this potential as $V(x,y) = -a(x^2+y^2)+b(x^2+y^2)^2$, where $x = |\mathfrak{Re}(\Phi)|$ and $y = |\mathfrak{Im}(\Phi)|$.

implying $\frac{1}{2}\phi_0^2 = \frac{m_H^2}{\lambda}$. Hence the new ground state of the Higgs field is written as

$$\Phi = \mathfrak{Re}(\Phi) + i\mathfrak{Im}(\Phi) = \begin{pmatrix} \phi_0 \\ \\ \phi_2 \end{pmatrix} + i\begin{pmatrix} \phi_1 \\ \\ \phi_3 \end{pmatrix} = \begin{pmatrix} v \\ \\ 0 \end{pmatrix}$$

Before the symmetry breaking, the Higgs is initially situated at a point of symmetry at the origin of the potential, $V(0) = 0$. This is an unstable point, and slight fluctuations in the vacuum push the Higgs down into an infinite number of possible degenerate ground states. Since they are degenerate, there is no preferred direction in the configuration space of the Higgs ground state, $\{\phi_0, \phi_1, \phi_2, \phi_3\}$, and the manner in which its ground state is chosen is seemingly random. This transition is known as the electroweak phase transition. Spontaneously, the Higgs has acquired its vev. The vev is computed using the relationship $v = \left(\frac{1}{\sqrt{2}G_F}\right)^{\frac{1}{2}}$ [8] where $G_F$ is the Fermi constant. With a measurement of $1.166371(6) \cdot 10^{-5}$ GeV$^{-2}$ for $G_F$ [9], this yields

$v \approx 246$ GeV. What are the consequences of this? In a certain manner, this symmetry breaking "sets the dials" for the Standard Model by defining new particle states in the universe; namely, the existence and mass-states of the gauge vector bosons.

The gauge fields $B_\mu$ and $W^a_\mu$ have what are known as flavor eigenstates, which will recombine to construct the $W^\pm$ and $Z^0$ bosons as mass eigenstates and a massless photon; this is all as a result of the broken symmetry. This can be seen by examining the Higgs Lagrangian together with the broken-symmetry Higgs state and the form of the covariant derivative. Now, the Higgs field can take on an excited state with excitation $v + h(x)$ at a spacetime point $x$. Rewriting the field as $\Phi = \begin{pmatrix} v + h(x) \\ \\ 0 \end{pmatrix}$ and applying $D_\mu$ will reveal the massive fields within the kinetic energy term.

$$(D^\mu \Phi)^\dagger (D_\mu \Phi) = \frac{1}{2}(\partial_\mu h(x))^2 + \frac{g_1^2 v^2}{4}(W^1_\mu)^2 + \frac{g_1^2 v^2}{4}(W^2_\mu)^2 + \frac{v^2}{4}(g_1 W^3_\mu - g_2 B_\mu)^2 + ...$$

The linear combinations $\frac{g_1^2 v^2}{4}\big((W^1_\mu)^2 + (W^2_\mu)^2\big)$ and $\frac{v^2}{4}(g_1 W^3_\mu - g_2 B_\mu)^2$ take the form of massive fields in the Lagrangian. Their existence in the Lagrangian puts them in direct correspondence with the existence of massive gauge fields for the $W^\pm$ and $Z^0$. The existence of the photon is consistent with the absence of such a mass term, which corroborates the theory so far. The vector boson states are given below.

$$Z_\mu = \cos\theta_w W^3_\mu - \sin\theta_w B_\mu$$

$$A_\mu = \sin\theta_w W^3_\mu + \cos\theta_w B_\mu$$

$$W^\pm_\mu = \frac{1}{\sqrt{2}}\Big(W^1_\mu \pm i W^2_\mu\Big)$$

$\theta_w$ is called the Weinberg angle or the weak mixing angle, given by $\tan\theta_w = \frac{g_2}{g_1}$. It

is a convenient parameterization of the mixing which illustrates the rotation of $W_\mu^a$ and $B_\mu$ into the massive fields. So, the mass eigenstates of the fields we see today are essentially a result of the $W_\mu^1$, $W_\mu^2$, $W_\mu^3$, and $B_\mu$ flavor $SU(2) \times U(1)$ eigenstates getting mixed via the Higgs mechanism.

## 1.2 Goldstone's Theorem

Through the transformation of the Higgs from its symmetric state to the symmetry-broken ground state, three degrees of freedom were apparently lost. Those are the $\phi_1$, $\phi_2$, and $\phi_3$ by the choice of basis. When a symmetry is broken in complex scalar field theory, these missing degrees of freedom usually become massless modes of oscillation called Goldstone bosons. Their existence is derived from Goldstone's theorem, a statement which is more mathematical than physical, and draws only from the group structure of the fields [5]. Ref. [3] is a seminal article which proves the Goldstone theorem.

However, what the Goldstone modes have done is placed themselves in a way so that 3 new massive fields have arisen; the $W_\mu^+$, $W_\mu^-$, and the $Z^0$ bosons. These three new fields, being massive, each have three polarization states now, whereas before they only had two when they were massless. The Higgs mechanism has given them a longitudinal state to add to their two transverse polarizations. The three Goldstone modes of the Higgs have placed their degrees of freedom in the longitudinal modes of the $W$ and $Z$ bosons [10],[6].

To see why the longitudinal modes of the vector bosons are consistent with their being massive, consider a general four-potential $B_\mu$. This potential satisfies the Proca wave equation for a massive spin-1 boson:

$$(\Box + m^2)B_\mu - \partial^\mu(\partial_\nu B^\nu) = 0; \quad \Box = \partial_\mu\partial^\mu$$

The solutions are of the form $A\epsilon^\mu e^{-ip_\mu x^\mu}$, where $A$ is a normalization constant and $\epsilon^\mu$ is the polarization vector. Taking another four-derivative of the Proca equation will yield the Lorenz condition;

$$\partial_\mu B^\mu = 0.$$

Substituting in the solution for $B^\mu$ into the Lorenz condition gives $p_\mu\epsilon^\mu = 0$. Using this fact obtains the form of the polarization vectors as

$$\epsilon^\mu = A\left(\frac{|\vec{p}|}{E}, \frac{\vec{p}}{|\vec{p}|}\right)$$

such that $p_\mu\epsilon^\mu = A(|\vec{p}| - |\vec{p}|) = 0$. Immediately, the left and right handed circular polarizations (helicities) for a boson traveling in the $z$-direction can be written down as linear combinations of $\epsilon^\mu_x$ and $\epsilon^\mu_y$:

$$\epsilon^\mu_+ = \frac{1}{\sqrt{2}}(0, 1, i, 0) \qquad\qquad \epsilon^\mu_- = \frac{1}{\sqrt{2}}(0, 1, -i, 0) \tag{1.2}$$

Putting in $\vec{p} = (0, 0, p_z)$ gives the longitudinal polarization vector

$$\epsilon^\mu_L = (A\frac{p_z}{E}, 0, 0, A).$$

In Minkowski space with signature $(+, -, -, -)$, the normalization condition implies that $B_\mu B^\mu = -1$, so using the wave solution with the above longitudinal polarization

normalizes the wave such that $A = \frac{E}{m}$. Here, $m$ is the mass of the field, given by $E^2 = p^2 + m^2$ in natural units. Now we can rewrite the longitudinal polarization state with the normalization;

$$B_L^\mu = \frac{1}{m}\begin{bmatrix} p_z \\ 0 \\ 0 \\ E \end{bmatrix} e^{-ipx}$$

Clearly, $m \neq 0$ if this state is to exist [2], [10].

Because the Goldstone modes of the Higgs field manifest themselves in the longitudinal modes of the massive vector bosons, examining interactions involving the longitudinal modes of the $W$ and $Z$ bosons is very direct way to scrutinize the effects of EWSB. Some processes of interest are $W_T W_L$ (transverse-longitudinal scattering), $W_L W_L$, and perhaps even $W_L Z_L$ scattering. This is especially of interest because without the Higgs boson, the longitudinal scattering of the vector bosons actually violates unitarity in the appropriate limit.

## 1.3 Unitarity

Unitarity in particle physics is commonly used as a guideline for deriving quantities and developing new models. Unitarity, being the preservation of probabilities, is in direct correspondence with the conservation laws of charge, energy, momentum, and so on. Violation of unitarity is as crucial a problem as the violation of any of the aforementioned, therefore unitarity becomes a strong fount of motivation for introducing new particles and interactions which preserve it.

The presence of the Higgs field with a nonzero vacuum expectation value allows the field to interact with other particles, the gauge vector bosons in particular. Allowing these interactions to happen rescues the Standard Model from scattering amplitudes which violate unitarity. This takes place in the longitudinal scattering of the vector bosons, where the amplitudes grow with energy. For example, the $s$ and $t$ channels for $WW$ scattering with the Higgs included as an interaction actually bring the total amplitude of $W_L W_L \to W_L W_L$ within the limit at which physics remains unitary; this is described using a unitarity bound.

The unitarity bound is an upper bound on the probability amplitude of a scattering process. This follows from the $S$-matrix, which is the time-evolution operator of scattering theory. Requiring that $\hat{S}^\dagger \hat{S} = 1$ places a bound on the amplitudes, which are proportional to matrix elements of $\hat{S}$. Writing $\hat{S} = 1 + i\hat{T}$, the matrix elements have that $i\mathcal{M} \propto iT_{fi}$ where $T_{fi}$ gives the transition probability from states $i$ to $f$. See appendix A.2 for further reference.

$\mathcal{A}(W_L W_L \to W_L W_L)$ can be broken up into a few diagrams: the $s$ and $t$ channels for $Z$ and $\gamma$, and the four-point $W$ diagram as shown in Figure 1.4. Recall that the Mandelstam variables [17] are combinations of the momenta as labeled in Figure 1.3:

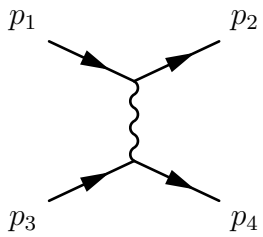


Figure 1.3: The momentum labeling convention for Mandelstam variables.

$$s = (p_1 + p_2)^2 = (p_3 + p_4)^2$$

$$t = (p_1 - p_3)^2 = (p_4 - p_2)^2$$

$$u = (p_1 - p_4)^2 = (p_3 - p_2)^2$$

The scattering amplitudes are [16]:

$$i\mathcal{M}_{WWWW} = i\frac{g_1^2}{4m_W^4}\Big(s^2 + 4st + t^2 - 4m_W^2(s+t) - \frac{8m_W^2}{s}ut\Big) \tag{1.3}$$

$$i\mathcal{M}_s^{\gamma+Z} = -i\frac{g_1^2}{4m_W^4}\Big(s(t-u) - 3m_W^2(t-u)\Big) \tag{1.4}$$

$$i\mathcal{M}_t^{\gamma+Z} = -i\frac{g_1^2}{4m_W^4}\Big(t(s-u) - 3m_W^2(s-u) + \frac{8m_W^2}{s}u^2\Big) \tag{1.5}$$

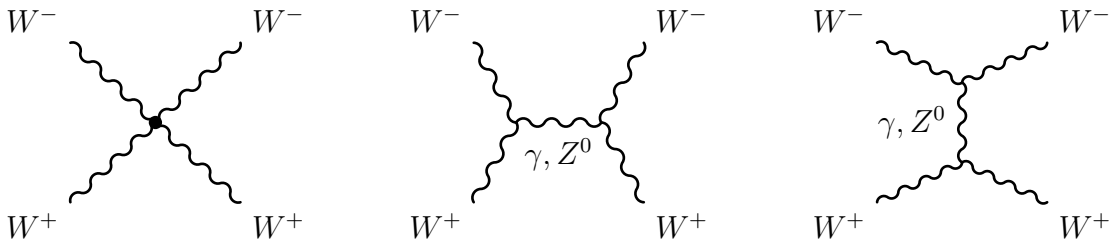


(a) 4-point $W$ (b) $s$-channel (c) $t$-channel

(Equation 1.3) (Equation 1.4) (Equation 1.5)

Figure 1.4: The possible $WW \to WW$ channels without the Higgs boson propagator.

Recall that $\sqrt{s} = E_{CM}$, the center of mass energy. Summing the matrix elements yields the total amplitude for $\mathcal{A}(W_L W_L \to W_L W_L)$, sans Higgs;

$$i\mathcal{M}^{\text{No Higgs}} = -i\frac{g_1^2}{4m_W^2}u + \mathcal{O}\big(\frac{E_{CM}}{m_W}\big)$$

This is linear in $u$ and violates the unitarity bound. Adding the Higgs diagrams (Figure 1.5) to the calculation of the amplitude will destroy this term;

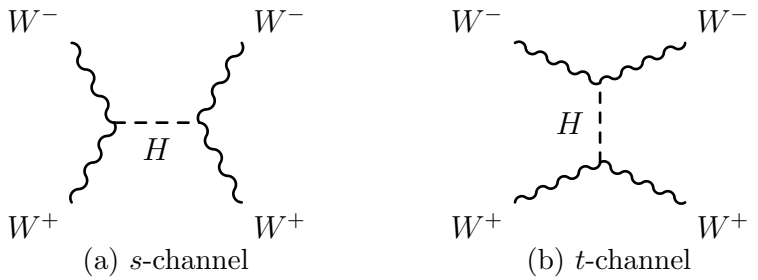


(a) $s$-channel (b) $t$-channel

Figure 1.5: The diagrams for $WW \to WW$ with the Higgs boson propagator.

$$i\mathcal{M}^{\text{Higgs}} = i\frac{g_1^2}{4m_W^4}u + \mathcal{O}\left(\frac{E}{m_W}\right)$$
$$\to i\mathcal{M}^{\text{Total}} = \mathcal{O}\left(\frac{E}{m_W}\right) = \mathcal{O}\left(\frac{\sqrt{s}}{m_W}\right)$$

and now the amplitude safely respects unitarity for $s \gg m_H^2, m_W^2$.

Refs. [11], [12], and [14] motivate the study of longitudinal "$W_L W_L$" processes with non-SM, or anomalous, couplings. Unitarity concepts similar to those presented above are key motivators for the derivation and analysis of the couplings as they apply to the gauge boson interactions, which will be discussed in the following chapter. The scattering of longitudinal $W$'s is a direct way of examining the effects of EWSB on couplings and particles beyond the Standard Model. Furthermore, we incorporate an electroweak dimension-6 model to examine anomalous couplings of the vector bosons using effective field theory (EFT) operators. The anomalous couplings are the low-energy effects of new physics, and they can be parameterized without having any explicit knowledge of a specific new physics model.

# 2

# Treating Anomalous Couplings with an Effective Field Theory

The Standard Model already includes many ways in which the fermion and boson fields can couple, or interact, with each other. Measuring signals from observables like the cross sections and transition rates of appropriate particle processes can indicate the strength of these couplings. Deviations from SM signals may be representative of new couplings called anomalous couplings, whose existence and nature are unconfirmed and considered to lie beyond the standard model, so we add them into the theory and gauge their effect on observables. The aim is to learn whether or not the anomalous couplings contribute anything to particle processes, and how strong the contributions may be if nonzero.

One way in which electroweak couplings can be described is through the electroweak Lagrangian, which directly describes the couplings. An alternative and less

direct method is through the use of vertex functions. Vertex functions are mathematical objects used in the calculation of probability amplitude matrix elements, and their functional forms are developed from Feynman rules. They are also designed to be unitary. For a good introduction to the calculation of matrix elements and deriving Feynman rules, see Ref. [10]. A strategy which is argued to be more economical and practical is effective field theory; Ref. [14] contrasts the Lagrangian method and the vertex function method against an EFT and demonstrates the usefulness of EFT.

Effective field theory is an approach to discovering new physics indirectly. While the direct approach might entail looking for evidence of new particles, this is very model specific and hinges on knowing the explicit Lagrangian associated with the new particles and interactions. An effective field theory is model independent, meaning that only the plausible effects of the new physics, in the form of anomalous couplings of SM particles, need to be known. Also, the EFT will come with free parameters which scale the effects of the new physics. So, if anomalous couplings do indeed give nonzero contributions, placing bounds on the EFT parameters will inform us about the constraints on those contributions. [14].

Our approach is as follows: parameterize the new physics by the characteristic mass or energy scale at which it appears, $\Lambda$. Recall that the SM Lagrangian has dimension 4, and so the effective Lagrangian begins at $n = 1$ corresponding to dimension $d = n + 4 = 5$. The effective Lagrangian that describes the new physics is a

double sum over the dimensions higher than 4 and the operators for each dimension.

$$\mathcal{L}_{EFT} = \sum_{n=1}^{\infty} \sum_{i} \frac{c_i^{(n)}}{\Lambda^n} \mathcal{O}_i^{(n+4)}$$

Here the coupling constants for each operator $\mathcal{O}_i^{(n+4)}$ are $c_i^{(n)}$.

The new physics operators should realize several important properties, including $S$-matrix unitarity, analyticity, and invariance under the full $SU(3)\times SU(2)\times U(1)$ gauge symmetry of the SM [11]. More relevantly, the Standard Model should be recovered in the low energy limit, i.e. when $\Lambda \to \infty$. In this sense, $\Lambda$ being the characteristic scale of the new physics, if the scale is high then the signal from anomalous couplings should vanish at low energies.

The goal is to look for the anomalous couplings as low-energy effects of the new particles. With this in mind, several steps can be taken to reduce the number of operators relevant to the analysis, chiefly following from Hagiwara's 1993 paper [15]. First, the operators involving fermion fields will have coupling constants on the order of the fermion masses. Since the fermion masses are small, the strength of the new operators will be negligible $[\mathcal{O}(\frac{m_f}{\Lambda})]$. So, the fermion operators can be ignored. Also, operators of dimension higher than $d = 8$ will only play a part at much higher energies. The only operators that should be examined are the ones that both deal with the EWSB sector and are the most relevant at low energies. Therefore we are interested in the electroweak dimension-6 operators.

## 2.1 The Operators

With these constraints we can focus on the dimension-6 terms given by $n = 2$.

$$\mathcal{L} = \mathcal{L}_{SM} + \sum_i \frac{1}{\Lambda^2}\mathcal{O}_i$$

These operators account for several types of interactions, including Higgs self-interactions, but we will focus on those that affect BSM triple gauge boson vertices. These are the following [12], [14], [15].

$$\mathcal{O}_{WWW} = \mathrm{Tr}[W_{\mu\nu}W^{\nu\rho}W^{\mu}_{\rho}] \tag{2.1}$$

$$\mathcal{O}_{W} = (D_\mu\Phi)^\dagger W^{\mu\nu}(D_\nu\Phi) \tag{2.2}$$

$$\mathcal{O}_{B} = (D_\mu\Phi)^\dagger B^{\mu\nu}(D_\nu\Phi) \tag{2.3}$$

$$\mathcal{O}_{\tilde{W}WW} = \mathrm{Tr}[\tilde{W}_{\mu\nu}W^{\nu\rho}W^{\mu}_{\rho}] \tag{2.4}$$

$$\mathcal{O}_{\tilde{W}} = (D_\mu\Phi)^\dagger \tilde{W}^{\mu\nu}(D_\nu\Phi) \tag{2.5}$$

Recall that $F_{\mu\nu}$ is the field strength tensor of electromagnetism, which contains the components of the $\vec{E}$ and $\vec{B}$ fields. The components of the tensor are $\partial_\mu A_\nu - \partial_\nu A_\mu$. Likewise, $B_{\mu\nu}$ is the field strength tensor for the $B_\mu$ gauge field, given by

$$B_{\mu\nu} = i\frac{g_2}{2}(\partial_\mu B_\nu - \partial_\nu B_\mu)$$

Since the $W^a_\mu$ fall under $SU(2)$ group action, not $U(1)$, their field strength tensor has an antisymmetry term;

$$W_{\mu\nu} = i\frac{g_1}{2}\sigma^a(\partial_\mu W^a_\nu - \partial_\nu W^a_\mu + g_1\epsilon_{abc}W^b_\mu W^c_\nu)$$

and we have to sum over $a = 1, 2, 3$ as well.

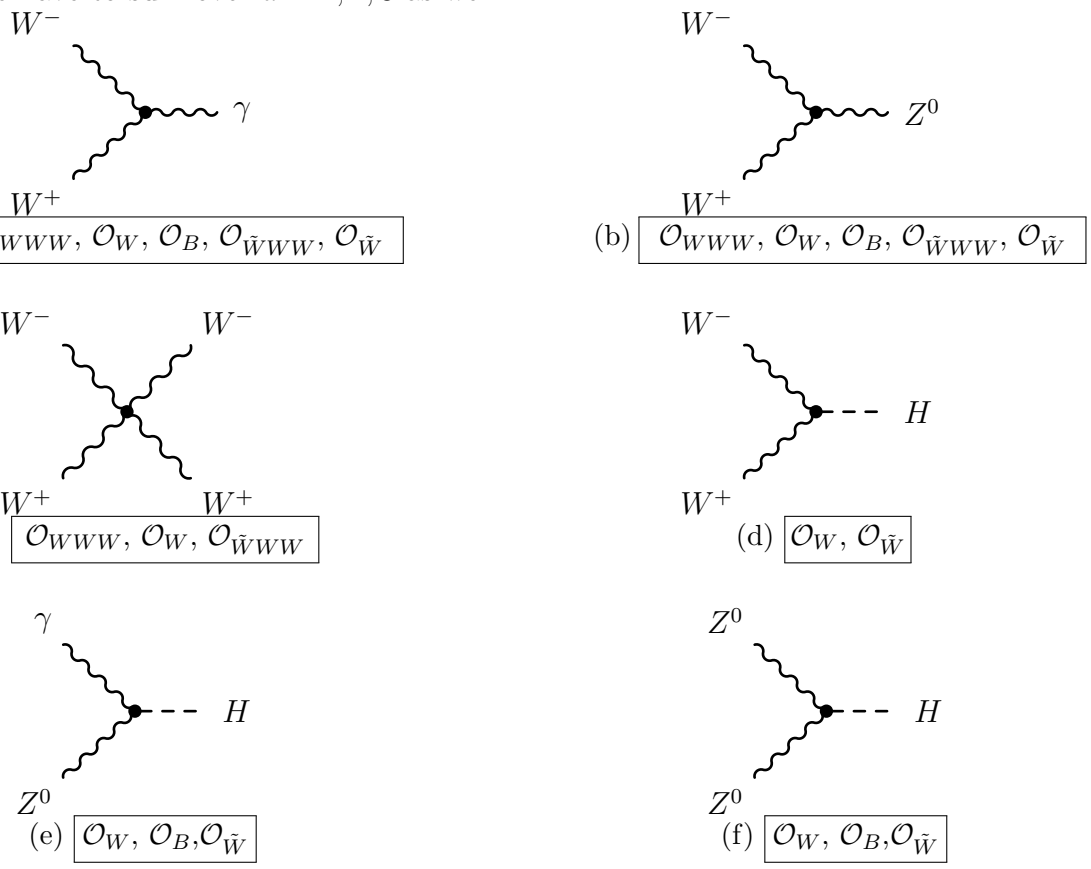


Figure 2.1: The vertices affected by the electroweak dimension-6 operators in equations 2.1-2.5. For a more complete list of vertices and the operators associated with them, see Ref. [12].

Each operator accounts for a number of possible interaction vertices, which are summarized in Figure 2.1. Since they involve the Higgs field $\Phi$ and the gauge field strength tensors, it is reasonable enough to expect that $\mathcal{O}_W$ and $\mathcal{O}_B$ account for interactions between the vector bosons and the Higgs boson, while $\mathcal{O}_{WWW}$ might account for $W$ self interactions, as they do in the figure. The operators to be mainly concerned with are the first three, $\mathcal{O}_{WWW}$, $\mathcal{O}_W$, and $\mathcal{O}_B$. The last two, $\mathcal{O}_{\tilde{W}WW}$

and $\mathcal{O}_{\tilde{W}}$ are not constrained to respect charge or parity conservation. Since weak interactions are known to exhibit charge or parity violations, there is no good reason to exclude $\mathcal{O}_{\tilde{W}WW}$ and $\mathcal{O}_{\tilde{W}}$ from the analysis, but the first three are highlighted to avoid being too general for this work.

An important nuance is the relationship between the dimension-6 operators and the boson helicity states. As a rule of thumb, operators that contain derivatives of the Higgs field, $D_\mu\Phi$, affect vertices with $W_LW_L$ states, while operators that contain the field-strength tensors $W_{\mu\nu}$ modify $W_TW_T$ state vertices. Hence, $\mathcal{O}_{WWW}$ purely affects $W_TW_T$ vertices, $\mathcal{O}_B$ affects purely $W_LW_L$ vertices and $\mathcal{O}_W$ affects all helicities [2]. This fact will be revisited in the analysis within Section 3.2.

The corresponding coupling constants for these operators are then $c_W$, $c_{WWW}$, $c_B$, $c_{\tilde{W}}$ and $c_{\tilde{W}WW}$. As an example, consider including only $\mathcal{O}_W$ in the EFT. The Lagrangian then becomes

$$\mathcal{L} = \mathcal{L}_{SM} + \frac{c_W}{\Lambda^2}\mathcal{O}_W.$$

With this model, the scattering diagrams which contain the vertices in Figure 2.1 have another contribution to the probability amplitude from the effective operators. Total amplitudes should sum over the diagrams with anomalous couplings where any dimension-6 operators included in the theory are active, as well as the diagrams with Standard Model vertices. In the case of dimension-6, all the operators contribute a terms proportional to $\frac{1}{\Lambda^2}$ to the amplitudes [14]. At particle energies higher than $\Lambda$ the dimension-8 operators, suppressed by a factor of $\Lambda^4$, contribute too strongly to the signal to be ignored; therefore the EFT for dimension-6 should only be valid up to

the scale of $\Lambda$. An important measure of this contribution will be the scattering cross section of VBS events; more specifically, the differential cross section with respect to the invariant pair mass of the pair-produced bosons will be examined in the next chapter.

## 2.2 Unitarity II

A natural question that arises is "How do the inclusion of the anomalous couplings through an EFT affect unitarity?" One might think that, like the vertex functions, the effective operators $\mathcal{O}_i$ are contrived such that they respect unitarity. The answer is no; effective field theory is a low energy theory, so it only needs to be valid at low energies (those below the characteristic scale $\Lambda$). The effective operators will be invalid anyway at energies far above the unitarity bound. Of course, unitarity should be respected in the range of energies for which the operators are valid, but it is irrelevant for energies beyond that point [14].

| Operator | Coefficient | 68% C.I. [TeV$^{-2}$][20] | 90% C.I. [TeV$^{-2}$][19] |
|---|---|---|---|
| $\mathcal{O}_{WWW}$ | $\frac{c_W}{\Lambda^2}$ | [-11.9, -1.94] | [-15, 3.9] |
| $\mathcal{O}_W$ | $\frac{c_{WWW}}{\Lambda^2}$ | [-8.42, 1.44] | [-5.6, 9.6] |
| $\mathcal{O}_B$ | $\frac{c_B}{\Lambda^2}$ | [-7.9, 14.9] | [-29,8.9] |
| $\mathcal{O}_{\tilde{W}WW}$ | $\frac{c_{\tilde{W}WW}}{\Lambda^2}$ | [-185.3, -82.4] | |
| $\mathcal{O}_{\tilde{W}}$ | $\frac{c_{\tilde{W}}}{\Lambda^2}$ | [-39.3, -4.9] | |

Table 2.1: Confidence intervals for the values of $\frac{c_i}{\Lambda^2}$ for each operator.

Confidence intervals (C.I.) of the effective operators' coefficients have been derived in Refs. [19] and [20]. These are confidence limits that are based on unitarity constraints; they are summarized in Table 2.1. This is a good indication of the range of values that the operator coefficients should take on, if they are present in the new physics.

# 3

# Experimental Processes and Methods

The new physics as discussed in the previous chapter, of which the underlying mechanisms are unknown, is best sought through the interactions of the gauge bosons. Through these interactions one can study the effects of the electroweak operators, as they contribute to probability amplitudes in many different and interesting ways. It is useful to perform a scattering experiment whose key observables (namely the cross section) will be affected by the presence of the EFT. VBS processes depend on the properties of the Higgs and serve as a means to study EWSB.

There are numerous ways that the Higgs interacts with Standard Model particles, and some of the most important ones are shown in Figure 3.1. In order to study BSM effects of EWSB, a focus is placed on $VV$ scattering, where $V = W^{\pm}, Z^{0}$. At higher beam energies, the cross sections of these events will demonstrate deviations from the

Standard Model by way of new couplings between the higgs and the vector bosons. With this concentration in mind, our task is now to elect a representative process of electroweak symmetry breaking from an appropriate set of particle interactions to test in simulation and subsequently analyze.

Processes which can produce a Higgs particle are automatically of interest because of the unitarizations that the Higgs boson provides. Some of the most important Higgs-producing diagrams are shown in Figure 3.1. A focus on EWSB restricts the Higgs channels to the electroweak sector. Gluon fusion (a), albeit the most abundant of the possible channels for Higgs production with the highest transition rate, is an example of an interaction with purely QCD couplings which do not tell us about EWSB. Hence, in our examination we absolutely neglect strong, or QCD, interactions. The processes of interest will include the production or annihilation of $W^{\pm}$ or $Z$ (d), which can decay leptonically or hadronically. For this reason, the Higgsstrahlung decay (b) and $t\bar{t}$ decay (c) channels cannot be neglected because they have the same signature decay products as in (d). Therefore they must be treated as irreducible backgrounds to the process of interest.

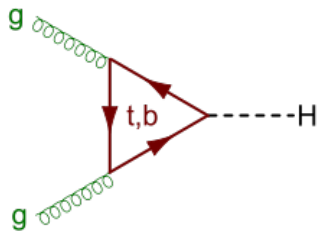


(a) Gluon Fusion. A loop of virtual quarks produces the Higgs.

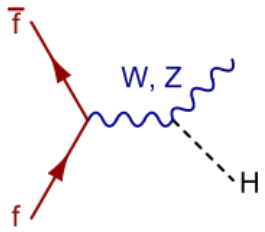


(b) Higgsstrahlung decay.

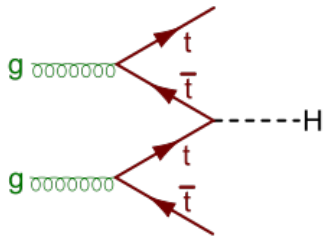


(c) Our principal source of backgrounds.

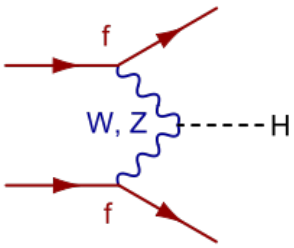


(d) Vector boson scattering

Figure 3.1: The dominant sources of Higgs production. Here f stands for fermion currents [25].

## 3.1 $WW$ Scattering

There are several motivations for studying $VV$ scattering, of which there are a few variations. One of the principal motivations to study these experimentally is to confirm or reject possible new physics of the Higgs boson. $WW \to WW$ becomes very important at high energies due to diagrams containing $HWW$ vertices, in which

unitarity becomes relevant. In this way, it is important to experimentally realize the exact cancellations of the divergences as seen in Section 1.3; otherwise, the Higgs particle found at the LHC may not be the SM Higgs that it was thought to be [12]. Furthermore, unitarity breaks down again in $WW$ scattering processes with center of mass energies above 1.2 TeV, so it is expected that BSM physics should play a role in canceling out the SM divergences there as well [2]. This is one of the key motivations for constraining the physics of anomalous couplings through an EFT, especially with the dimension-6 operators chosen. $WW \to WW$ diagrams will include many of the vertices affected by the electroweak dimension-6 operators, and while they don't play a role in preserving unitarity at the low-energy scale of the EFT, gauging the contribution of each vertex will be indicative of how those couplings might rescue unitarity in the TeV range.

Longitudinal scattering processes, $W_L W_L \to W_L W_L$, as opposed to purely transverse scattering ($W_T W_T \to W_T W_T$), dominate at high energies. This fact is explicated by the forms of the vector boson polarization states derived in Section 1.2;

$$\epsilon_+^\mu = \frac{1}{\sqrt{2}}(0,1,i,0) \qquad \epsilon_-^\mu = \frac{1}{\sqrt{2}}(0,1,-i,0) \qquad \epsilon_L^\mu = \frac{1}{m_W}(p_z,0,0,E) \tag{3.1}$$

The polarization $|\epsilon_L^\mu|$ grows with $E$, and as $E$ overpowers the $W$ mass, the probability for $W_\mu^\pm$ to be in the longitudinal state will grow much larger than the amplitudes for the transverse polarizations. This growth is unbounded and is reason enough to worry about unitarity in $WW \to WW$, but just as demonstrated in Section 1.3, the contributions to the probability amplitude from the Higgs coupling cancel out the

divergences. The Higgs not only takes care of unitarity in the $W_LW_L \to W_LW_L$ case, but also in $W_LZ_L \to W_LZ_L$ and $Z_LZ_L \to Z_LZ_L$ processes.

So, with $W_LW_L$ as the focus, what decay channels are available in experiment to choose from, and which one is optimal? Each final state $W$ is capable of decaying into a lepton and lepton-neutrino pair, or a quark-antiquark pair. Hence, the possibilities are dileptonic channel ($WW \to WWl\nu_l l\nu_l$), semi-leptonic channel ($WW \to WWl\nu_l q\bar{q}$), and purely hadronic channel ($WW \to WWq\bar{q}q\bar{q}$). The benefits and downsides of each channel are weighed to make the analysis as easy as possible while providing the highest possible yield in relevant particle data.

An analysis of each decay channel of the final state $W_LW_L$ pair follows, beginning with the dileptonic channel (Figure 3.2). Recall that the branching ratio

$$BR_{mode} = \frac{\Gamma_{mode}}{\Gamma}$$

indicates how often a given mode occurs in a large enough sample of scattering events.

The dileptonic channel would ordinarily be the "gold plated" choice [11], since the purely leptonic decay cannot be mistaken for any QCD backgrounds. However, the branching ratio is quite small, lying at 10.60%. Also, the neutrino pair in this decay mode is a source of ambiguity; neutrinos, being practically massless and noninteracting, pass easily through detectors. This creates a gap in the kinematics in the form of missing momentum and energy during the reconstruction of the $W$ invariant pair mass, a method detailed in Appendix A.3. The sum of the decay products' momenta should equal that of the $W$ pair due to conservation. To

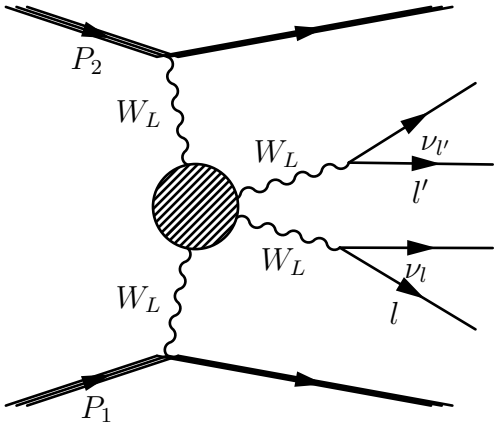


Figure 3.2: Dileptonic decay channel. The blob in the center "vertex" represents both the $t$ and $s$ channel possibilities for $A, W, Z$, or $H$ exchange, with the possible inclusion of any anomalous coupling vertex.

account for the missing neutrino momentum, let the total neutrino momentum equal the negative sum of the measured momenta so that the total momentum is zero in the rest frame; $p^{\mu}_{miss} = -\sum p^{\mu}_{detected}$. If there is more than one neutrino, however, then the unknown momentum distribution among the neutrinos makes the distribution of momenta among the parent $W$'s unknown. This is a crucial disadvantage of the dileptonic decay channel.

The examination turns to hadronically decaying $W$'s, seen in Figure 3.3. This channel is unfavorable mainly because the purely hadronic decay products have many QCD backgrounds coming from other jet sources. While it does have the highest branching ratio of 45.70%, the ratio of signal events to background events is too small for this process to be useful.

The last mode to discuss is the semileptonic $l\nu q\bar{q}$ decay channel (Figure 3.4). Here,

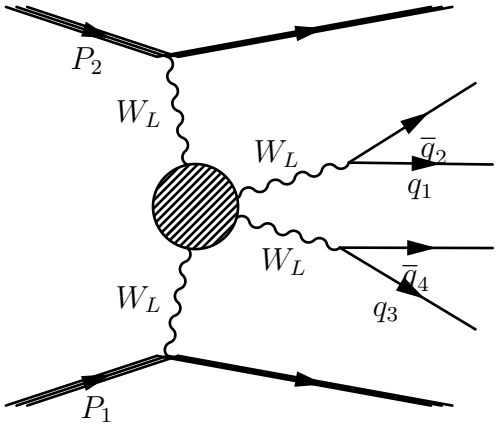


Figure 3.3: Hadronic decay channel

missing momentum from the single neutrino can be accounted for; quark production in this diagram does produce jets, but these can be distinguished, or "tagged," from other hadronic jets through the $W$-jet tagging method [18]. This method identifies the hadronically decaying $W$ bosons by unique qualities of the jet substructure of the $W$-jets. There is only a slight trade-off in the branching ratio, which still small (44.04%), but the semileptonic channel is still completely accessible kinematically. Together, these reasons make the semileptonic channel the most favorable channel to study. Table 3.1 summarizes the positive and negative qualities of the $WW$ decay channels.

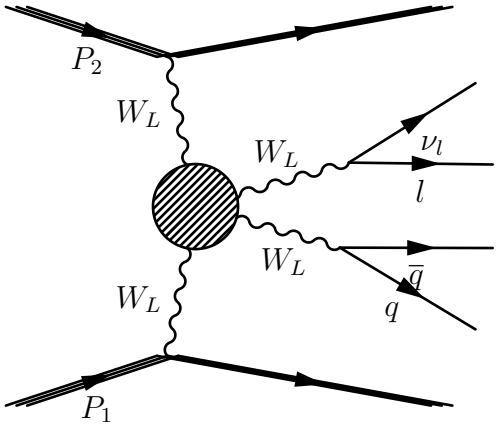


Figure 3.4: Semileptonic decay channel

| Decay | Branching Ratio (%) | Pros | Cons |
|---|---|---|---|
| $l\nu_l l\nu_l$ | $10.60 \pm 0.96$ | No QCD Bkg | Ambiguous $E_{miss}$, Low B.R. |
| $l\nu_l q\overline{q}$ | $44.04 \pm 1.50$ | Accountable $E_{miss}$ | QCD Bkg |
| $q\overline{q}q\overline{q}$ | $45.70 \pm 0.54$ | High B.R. | QCD Bkg |
| | | | B.R. = branching ratio |
| | | | bkg = backgrounds |

Table 3.1: Branching ratios calculated from those for the decay modes of the $W$'s, taken from the Particle Data Group [23].

## 3.2 Measurement of dimension-6 contributions

A strong measure of the contributions of the EFT relative to those of the Standard Model is the differential cross section. A common way to see the differential cross section is with respect to the solid angle $\Omega$, as $\frac{d\sigma}{d\Omega}$. However, the differential cross

section is also proportional to the number of scattering events, or interactions; in this sense, it is useful to see how the cross section varies with respect to many other kinds of variables. In the following analysis, we will inspect the differential cross section for a $WW$ scattering process as a function of the invariant mass of the $W$ pair. Referring back to Figure 3.4, this will be the pair mass reconstructed from the $l\nu q\bar{q}$ decay products.

Here a focus will be on the operators $\mathcal{O}_W$, $\mathcal{O}_B$, and $\mathcal{O}_{WWW}$. As mentioned in Chapter 2, the operators affect $WW$ scattering differently for each polarization state, an effect that becomes clear in the cross-sectional distributions. Since $W_L$ production dominates at higher energies, the presence of $\mathcal{O}_B$ in the effective Lagrangian, which only affects $W_L$ vertices, will have the bulk of its impact on the cross section at high mass. Meanwhile $\mathcal{O}_{WWW}$, only affecting $W_T$ interactions, is expected to have a dominant effect towards the low-mass end of the differential cross section distribution.

The distributions in Figure 3.5 were taken from Michał Szleper's brilliant exposé on $WW$ scattering, Ref. [2]. They were developed using the particle simulation Monte Carlo MadGraph [21]. The top two graphs in the figure present the effects the effective operators on the $W_LW_L$ cross section for different values of $\frac{c_W}{\Lambda^2}$ and $\frac{c_B}{\Lambda^2}$. Notice that positive and negative values of $\frac{c_W}{\Lambda^2}$ and $\frac{c_B}{\Lambda^2}$ introduce interference around the order of $\Lambda$ in the $WW$ mass, which is consistent with the functional form of the differential cross section when dimension-six anomalous couplings are included. The same interference occurs in the $W_TW_L$ and $W_TW_T$ cross sections, but this time much more suppressed.

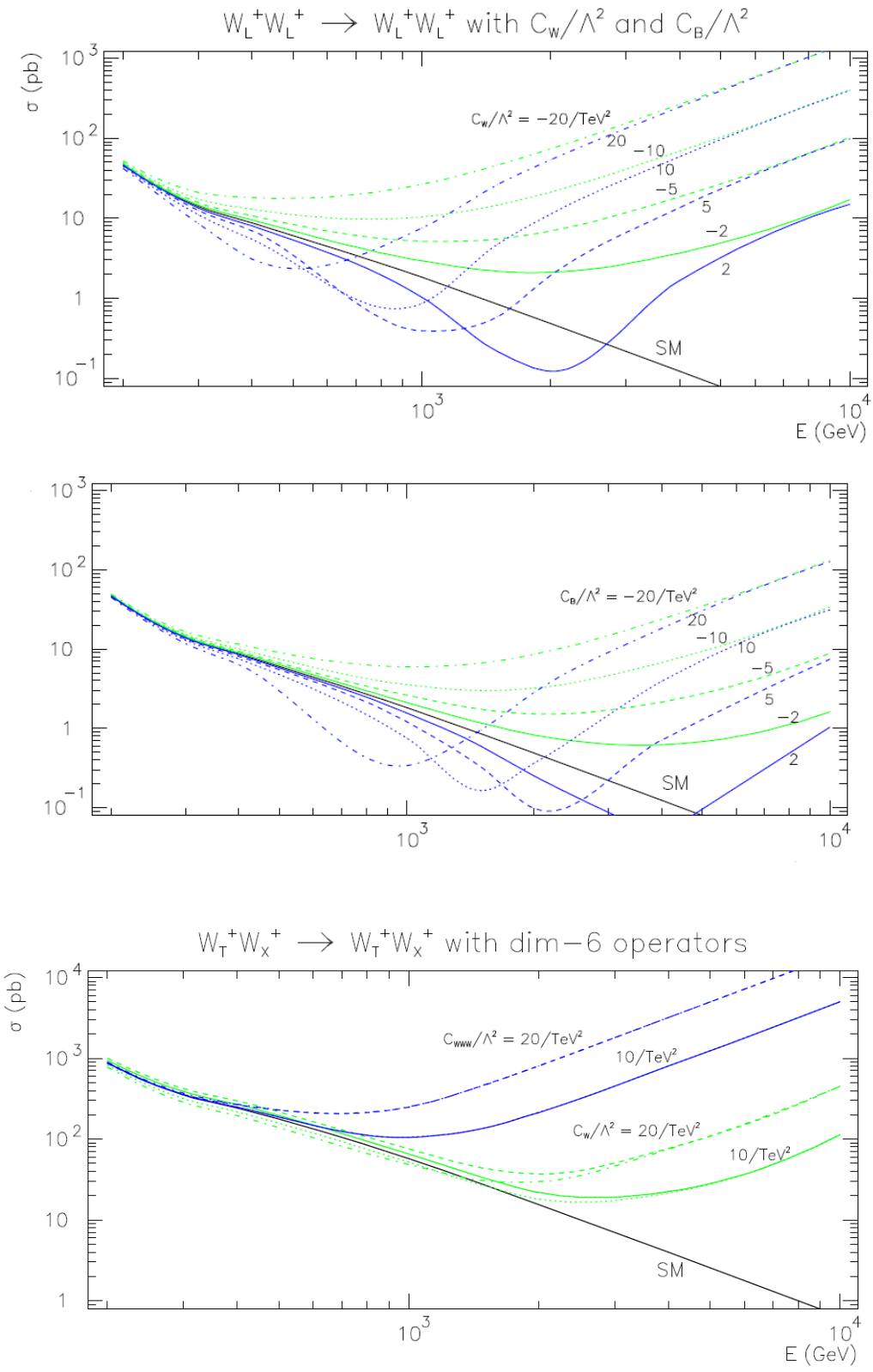


Figure 3.5: SM and SM + EWdim6 cross sections with various values of the dimension-6 couplings [2]. Compare these to the forms in equations 3.2-3.7.

The functional forms for $WW$ scattering differential cross sections of every helicity combination are listed in equations 3.2 - 3.7, with the order of the terms always arranged as SM + Interference + Dimension-6 [12], [13]. Expressed as functions of $s = E_{CM}^2$, they are derived from the functional forms of the sum of the squares of the matrix elements, which are proportional to the differential cross sections. Notice that the interference term must be proportional to the negative of the dimension-6 coupling constant in order to be consistent with the positive interference ($\frac{c_i}{\Lambda^2} < 0$) or destructive interference ($\frac{c_i}{\Lambda^2} > 0$) in Figure 3.5.

$W_L W_L$:

$$\frac{d\sigma}{dm_{WW}} \propto \underbrace{\frac{\Lambda}{s}}_{SM} - \underbrace{\frac{c_i}{\Lambda^2}}_{Interference} + \underbrace{\frac{s}{\Lambda^4}}_{Dimension-6} \qquad \mathcal{O}_B, \mathcal{O}_W \qquad (3.2)$$

$$\frac{d\sigma}{dm_{WW}} \propto \underbrace{\frac{\Lambda}{s}}_{SM} \qquad \mathcal{O}_{WWW} \qquad (3.3)$$

$W_L W_T$:

$$\frac{d\sigma}{dm_{WW}} \propto \frac{\Lambda}{s^2} - \frac{c_i}{s\Lambda^2} + \frac{1}{\Lambda^4} \qquad \mathcal{O}_B, \mathcal{O}_W, \mathcal{O}_{WWW} \qquad (3.4)$$

$W_T W_T$:

$$\frac{d\sigma}{dm_{WW}} \propto \frac{\Lambda}{s} - \frac{c_i}{s\Lambda^2} + \frac{s}{\Lambda^4} \qquad \mathcal{O}_{WWW} \qquad (3.5)$$

$$\frac{d\sigma}{dm_{WW}} \propto \frac{\Lambda}{s} - \frac{c_i}{s^2\Lambda^2} + \frac{1}{s\Lambda^4} \qquad \mathcal{O}_W \qquad (3.6)$$

$$\frac{d\sigma}{dm_{WW}} \propto \frac{\Lambda}{s} \qquad \mathcal{O}_B \qquad (3.7)$$

An attempt to reproduce the effects of the EW dimension-6 operators $\mathcal{O}_{WWW}$ and $\mathcal{O}_W$ was made using MadGraph 5, the results of which are in Figures 3.6 and 3.7.

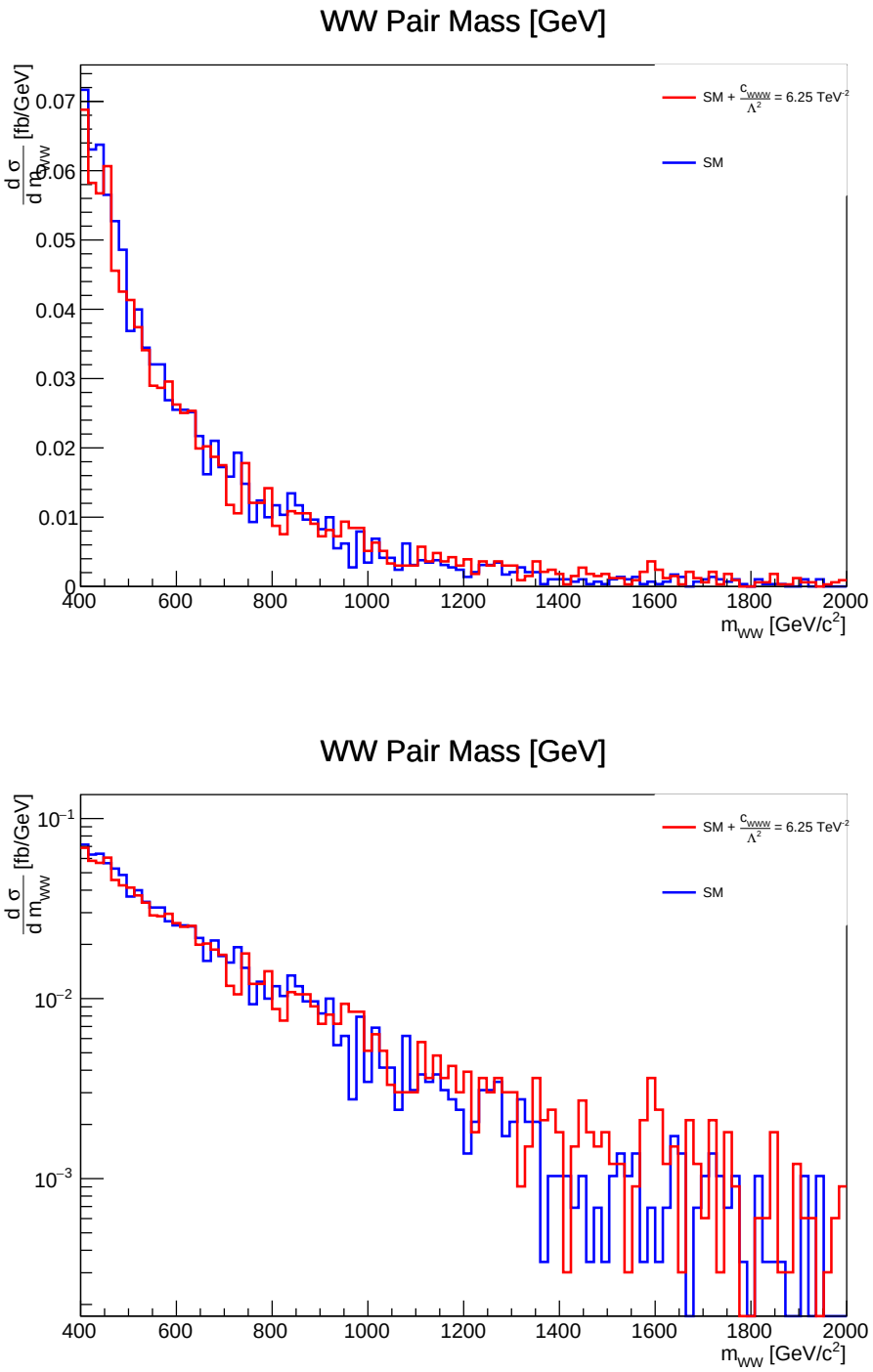


Figure 3.6: MadGraph results of the comparison between the SM and SM + $\mathcal{O}_{WWW}$ ($\frac{c_{WWW}}{\Lambda^2}$ = 6.25 TeV$^{-2}$, corresponding to $\Lambda$ = 400 GeV) differential cross section for $pp \to WWjjl\nu q\overline{q}$. 10,000 events were generated with a center of mass beam energy of 14 TeV. Difference between the two is marginal and only seen within the log plot at high mass, indicating that the dimension-6 contribution is not fully integrated into the signal. $\sigma_{SM} = 0.4971 \pm 0.0014$ pb, $\sigma_{\mathrm{SM}+\mathcal{O}_{WWW}} = 0.5417 \pm 0.0014$ pb.

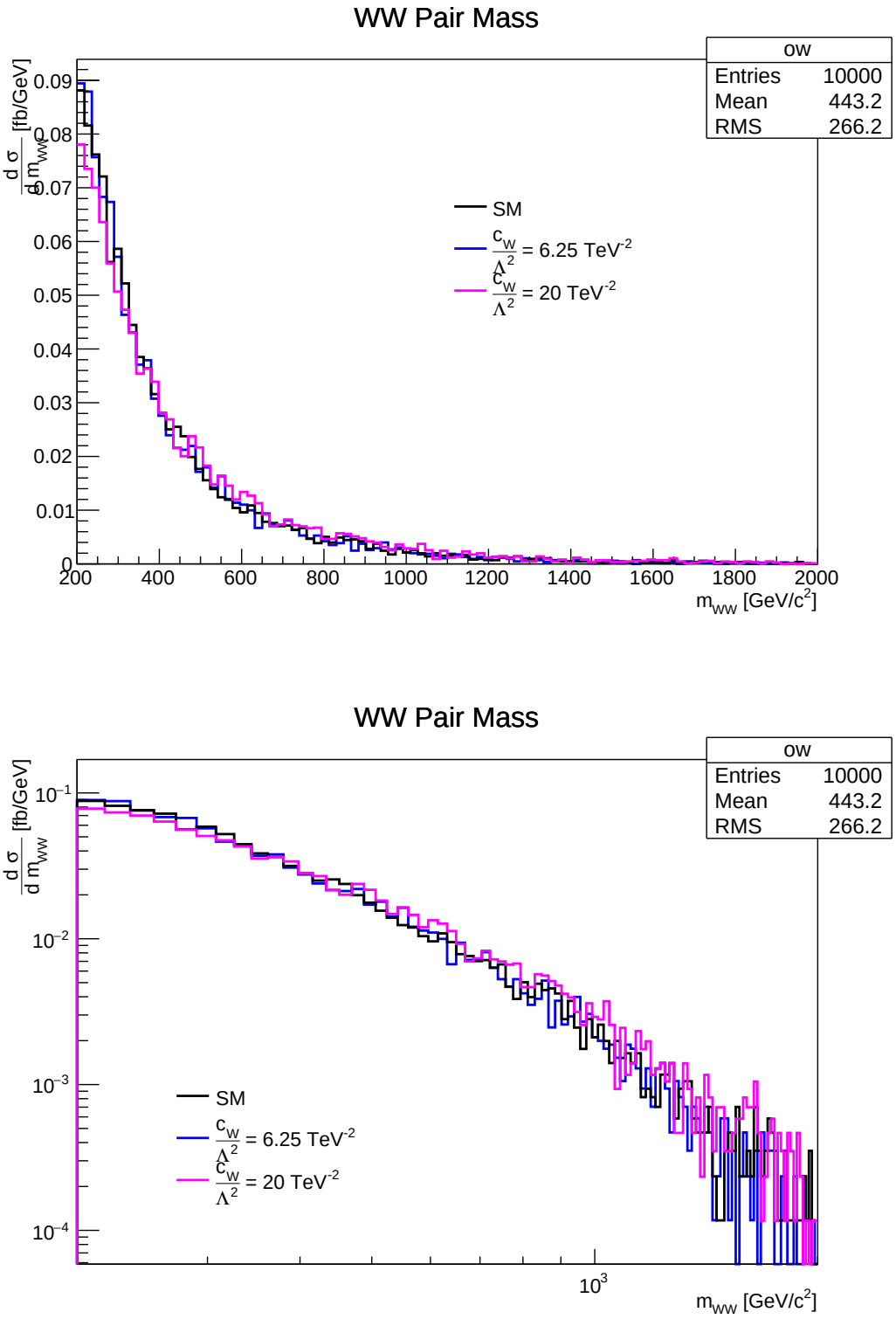


Figure 3.7: SM and SM + $\mathcal{O}_W$ comparison, with an accompanying double-log plot to illustrate the subtle differences. One can notice slight interference in the low-mass region where the SM cross signal overtakes that of the SM + $\mathcal{O}_W$, which is consistent with Figure 3.5. However, this effect is again far smaller than what we expect.

This compares the SM to the SM + $\mathcal{O}_{WWW}$ and SM + $\mathcal{O}_{W}$ signal, respectively. While there is an effect on the total cross section, not enough variation in the high-mass tail was observed. A better route may be to use VBFNLO (Vector Boson Fusion at Next to Leading Order [22]), which may handle the matrix element calculations of the triple gauge boson vertices more accurately.

If further analysis were to be performed, it is suggested that the functional forms in equations 3.2-3.7 should be verified with simulated data. Using the unitarity bounds in Table 2.1 as a guideline, one could perform a linear regression on a sufficiently reliable and large number of events with the electroweak dimension-6 operators incorporated. Additionally, Ref. [14] claims that $c_{WWW} < (4\pi)^2$, and other bounds can be placed on each $c_i$ via convergence of the perturbation expansion of matrix elements. With bounds placed on the coupling constants, fits could be obtained on the values of $c_W$, $c_{WWW}$, $c_B$, $c_{\tilde{W}}$, and $c_{\tilde{W}WW}$. This would be a good step towards gaining an intuition for what to expect from the new electroweak physics, if these couplings present themselves as nonzero contributions.

# 4

# Conclusion

Experimentally, particle physics is attaining deeper and deeper insights into physics beyond the Standard Model, well into the energy range of symmetry breaking. There are many opportunities to reveal new physics associated with the Higgs mechanism and EWSB grow, especially in high energy vector boson interactions.

Effective field theory is regarded as a powerful tool for efficient analysis in particle physics research. Wielding this technique as a method for discovery of new physics is beneficial for several reasons, chiefly because it is model independent and allows nature to make an appearance in whatever way it chooses. Particle physics simulations that incorporate an EFT model will provide a preliminary idea of where to look for the new physics. It opens the door to any kind of phenomena that we may look forward to, whether they enter in the form of new couplings, extra dimensions, or exotica.

# Appendix A

# Mathematical Tools

## A.1 Particle Symmetry Groups

Group theory in particle physics provides a way to get a birds-eye-view of the different species of particles and their properties. A *group* is a set, whose elements can be combined via a binary operation. A group remains closed under said operation, possesses an identity element, and inverse elements. A group can have an *action* on another set of elements, typically elements that maintain a symmetry when acted on by the elements of the group. For example, the group $D_{12}$ contains the 60° rotations about an axis and two reflections; a hexagon is symmetric under $D_{12}$ group action. In particle physics, it is the Lagrangian that is invariant under the group action on the particle wavefunctions. Some common groups are summarized below.

- $O(3)$ - the group of rotations in $\mathbb{R}^3$, represented by orthogonal $3 \times 3$ matrices.

- $SU(2)$ - the group of *special* ($\det U = 1$) *unitary* ($U^\dagger U = 1$) $2 \times 2$ matrices. Bosonic symmetries and electroweak theory are described by $SU(2)$.

- $U(1)$ - group of unitary transformations, whose elements can be represented by $e^{i\phi(x)}$. The symmetries of electromagnetism are described by $U(1)$.

- $SU(3)$ - represented by special unitary $3 \times 3$ matrices, and describes the symmetries of quarks and QCD.

- Lorentz Group and $SL(2,\mathbb{C})$ - The Lorentz group is the group generated by any combinations of the 3 boosts, $K_i$, and 3 rotations, $J_i$, as Lorentz transformations in spacetime. This group has a surjective correspondence, called a homomorphism, with the group of special linear, complex-valued $2 \times 2$ matrices $SL(2,\mathbb{C})$. Manifested as $SL(2,\mathbb{C})$, this group describes the Dirac theory of the electron.

- Poincaré - Regarded as the fundamental group of particle physics, the Poincaré group contains the Lorentz group plus transformations in space and time. Ref. [5] contains an in-depth discussion on these two groups.

## A.2 $S$-matrix

For a general time-evolution operator $\hat{U}(t_2, t_1)$ which carries a particle state from time $t_1$ to $t_2$ via $\hat{U}\,|\psi(t_1)\rangle = |\psi(t_2)\rangle$, the differential equation

$$i\frac{d}{dt_2}\hat{U}(t_2, t_1) = \hat{H}(t_2)\hat{U}(t_2, t_1)$$

implies that

$$\hat{U} = e^{-i\int_{t_1}^{t_2} dt\hat{H}(t)}.$$

In a particle physics scattering experiment, definite initial particle states at $t = -\infty$ are scattered into definite final particle states $t = \infty$. The time evolution operator that transforms the set of states $\{\Psi_i\}$ into $\{\Psi_f\}$ is the scattering matrix $\hat{S} = \lim_{t_1\to-\infty,t_2\to\infty} \hat{U}(t_2, t_1)$. The same properties of a general time-evolution operator apply; $\hat{S}^\dagger\hat{S} = 1$, and $|\{\Psi_f\}\rangle = \hat{S}\,|\{\Psi_i\}\rangle$. $\hat{S}$ has the solution

$$\begin{aligned}
\hat{S} &= T\Big[\exp\big(-i\int_{-\infty}^{\infty} dt\hat{H}(t)\big)\Big] \\
&= T\Big[\exp\big(-i\int_{-\infty}^{\infty} d^4x\hat{\mathcal{H}}(x)\big)\Big] \\
&= T\Big[\underbrace{1}_{free} \underbrace{-i\int d^4x\hat{\mathcal{H}}(x) - \frac{1}{2}\int d^4yd^4z\hat{\mathcal{H}}(y)\hat{\mathcal{H}}(z) + \ldots}_{interacting}\Big].
\end{aligned} \tag{A.1}$$

$\hat{H}(t)$ is replaced with the Hamiltonian spacetime density $\hat{\mathcal{H}}(x)$, and all products of $\hat{\mathcal{H}}$ must be ordered by later times (left) to earlier times (right) via $T[\ ]$. They must be ordered because the Hamiltonian doesn't always commute. Equation A.1 is called the Dyson expansion of $\hat{S}$. Consequently, the scattering matrix has the form

$$\hat{S} = 1 + i\hat{T}$$

where $\hat{T}$ is the transition matrix. $S$-matrix unitarity places a special condition on $\hat{T}$, which will be useful determining the unitarity bound of key observables such as the

cross-section and transition rate. Writing $\hat{T} = \mathfrak{Re}\hat{T} + i\mathfrak{Im}\hat{T}$,

$$\begin{aligned} 1 = \hat{S}^\dagger\hat{S} &= (1 + i\hat{T})^\dagger(1 + i\hat{T}) \\ &= (1 - i\hat{T}^\dagger)(1 + i\hat{T}) \\ &= 1 + i\hat{T} - i\hat{T}^\dagger + \hat{T}^\dagger\hat{T} \\ &= 1 + i\mathfrak{Re}\hat{T} - \mathfrak{Im}\hat{T} - i\mathfrak{Re}\hat{T} - \mathfrak{Im}\hat{T} + \hat{T}^\dagger\hat{T} \\ &= 1 - 2\mathfrak{Im}\hat{T} + \hat{T}^\dagger\hat{T}. \\ \rightarrow \hat{T}^\dagger\hat{T} &= 2\mathfrak{Im}\hat{T} \end{aligned}$$

This becomes particularly useful when using partial wave amplitudes to determine the scattering cross-section. The partial amplitudes are fractions of the total scattering amplitude, so their transition matrices must leave $\hat{S}^\dagger\hat{S} < 1 \rightarrow \hat{T}^\dagger\hat{T} < 2\mathfrak{Im}\hat{T}$. Through the relationship to the invariant matrix element $\mathcal{M}$,

$$\langle p_1 p_2 ... p_n | \, i\hat{T} \, | q_1 q_2 ... q_m \rangle = i\mathcal{M}(2\pi)^4\delta^4\bigg(\sum_i^n p_i - \sum_j^m q_j\bigg),$$

one can derive the **Optical Theorem**:

$$\mathfrak{Im}\mathcal{M} = 2E_{\mathrm{CM}}P_{\mathrm{CM}}\sigma$$

thereby relating the transition matrix to the total cross section $\sigma$.

## A.3 Momentum Reconstruction

Consider a single particle decaying into a set of $N$ final state particles. Momentum conservation in four dimensional spacetime imposes equivalence between the initial

state particle momentum $P_\mu$ and the final state momenta $p_\mu$;

$$P_\mu = \sum_{i=1}^{N} p_\mu^i.$$

The invariant mass $P_\mu P^\mu = E^2 - p^2 = m^2$ of the initial state can be reconstructed by squaring the R.H.S.;

$$m^2_{\text{initial}} = P_\mu P^\mu = \left( \sum_{i=1}^{N} p_\mu^i \right)^2.$$

In the case of a $1 \to 2$ process, the invariant mass is

$$m^2_{\text{initial}} = \eta_{\mu\nu}(p_1^\mu p_1^\nu + p_2^\mu p_2^\nu + 2p_1^\mu p_2^\nu) \tag{A.2}$$

$$= m_1^2 + m_2^2 + 2(E_1 E_2 - \vec{p_1} \cdot \vec{p_2}) \tag{A.3}$$

which is equivalent to taking the invariant "pair mass" of the 1 and 2 particles. This easily generalizes to a set of $M$ initial-state particles.

# Bibliography

[1] Espriu, Domènec and Yencho, Brian. Longitudinal $WW$ scattering in light of the "Higgs boson" discovery. Phsy. Rev. D. **87** 055017 (2013)

[2] Szleper, Michał. The Higgs boson and the physics of WW scattering before and after Higgs discovery. arXiv:1412.8367v2 [hep-ph] (2015)

[3] Goldstone, Jeffery. and Salam, Abdus. and Weinberg, S. Broken Symmetries. Phys. Rev. **127**, 965 (1962)

[4] Higgs, Peter W. Broken Symmetries and the Masses of Gauge Bosons. Phys. Rev. **13**, 508 (1964)

[5] Ryder, Lewis H. 1985, *Quantum Field Theory*, Cambridge University Press, Cambridge. Print.

[6] Lancaster, Tom, and Blundell, Stephen. 2014, *Quantum Field Theory for the Gifted Amateur*, Oxford University Press, Oxford. Print.

[7] Penrose, Roger. 2005, *The Road to Reality: A Complete Guide to the Laws of the Universe*, New York: A.A. Knopf. Print.

[8] Tilmen, Plehn and Rauch, Michael. Quartic Higgs Coupling at Hadron Colliders. Phys. Rev. D. **72** 053008 (2005)

[9] Chitwood, D.B. *et al.*. Improved Measurement of the Positive-Muon Lifetime and Determination of the Fermi Constant. Phys. Rev. **99**, 032001 (2007)

[10] Thomson, Mark. 2013, *Modern Particle Physics*, Cambridge University Press, Cambridge. Print.

[11] Cui, Yanou and Han, Zhenyu. New light on $WW$ scattering at the LHC with $W$ jet tagging. Phys. Rev. D. **89**, 015019 (2014)

[12] Degrande, Celine, Eboli, Oscar. Monte Carlo tools for studies of non-standard electroweak gauge boson interactions in multi-boson processes: A Snowmass White Paper. arXiv:1309.7890v1 [hep-ph] (2013)

[13] Degrande, Celine. BSM constraints from EW measurements. arXiv:1302.1112v1 [hep-ph] (2013)

[14] Degrande, Celine, Greiner, Nicolas. Effective Field Theory: A Modern Approach to Anomalous Couplings. arXiv:1205.4231v1 [hep-ph] (2012)

[15] Hagiwara, Kaoru., Ishihara, Sumio. Low energy effects of new interactions in the electroweak boson sector. Phys. Rev. D. **48**, 5 (1993)

[16] Cheung, Kingman. "WW Scattering." Duke Workshop: Electroweak Measurements at the Energy Frontier (2011): n. pag. Cern. Indico. Web. 19 May 2015.

[17] Mandelstam, Stanley. Determination of the Pion-Nucleon Scattering Amplitude from Dispersion Relations and Unitarity. Phys. Rev. **112**, 1344 (1958)

[18] Cui, Yanou and Han, Zhenyu and Schwartz, Matthew D. $W$-jet tagging: Optimizing the identification of boosted hadronically-decaying $W$ bosons. Phys. Rev. D. **83** 074023 (2011)

[19] Corbett, Tyler and Eboli, Oscar., and Gonzalez-Garcia, M. Unitarity Constraints on Dimension-six Operators. arXiv:1411.5026 [hep-ph]. (2014).

[20] "Models/EWdim6 - MadGraph." `https://cp3.irmp.ucl.ac.be/projects/madgraph/wiki/Models/EWdim6` MadGraph, Web.

[21] Alwall, Johan and Herquet, Michel and Maltoni, Fabio and Mattelaer, Olivier and Stelzer, Tim. MadGraph 5: going beyond. Journal of High Energy Physics **2011** 128. (2011)

[22] Arnold, Ken. *et al.* VBFNLO: A parton level Monte Carlo for processes with electroweak bosons. arXiv:0811.4559v2 [hep-ph]. (2009)

[23] J. Beringer et al. (Particle Data Group), PR **D86**, 010001 (2012) `http://pdg.lbl.gov`

[24] Georgia State University, *Hyperphysics*. Big Bang Expansion and the Fundamental Forces. `http://hyperphysics.phy-astr.gsu.edu/hbase/astro/unify.html`. Web.

[25] Rias, Timothy. By TimothyRias (Own work) [CC BY-SA 3.0 http://creativecommons.org/licenses/by-sa/3.0], via Wikimedia Commons